Task-Driven Subspace Decomposition for Knowledge Sharing and Isolation in LoRA-based Continual Learning

Lingfeng He, De Cheng, Huaijie Wang, Xi Yang, Nannan Wang, Xinbo Gao

Xidian University, Xi'an, China

INTRODUCTION & MOTIVATION

Problem Definition. **Continual Learning (CL)** studies how a model can continuously acquire new knowledge while retaining previously learned capabilities. **LoRA-based CL** has gained increasing attention due to the efficiency and scalability of LoRA.

Existing Solutions: They explicitly **isolate task-specific LoRA update subspaces via orthogonal constraints** to reduce cross-task interference.

Limitations: (1) They **discard transferable directions across tasks**, suppressing inter-task knowledge sharing; (2) Orthogonal constraints ensure a "safe zone" but **fail to find truly specific directions for new tasks**.

A Key Question: *How to **properly configure LoRA subspaces** in CL to preserve shared directions while learning truly task-specific knowledge, achiving better stability-plasticity trade-off?*

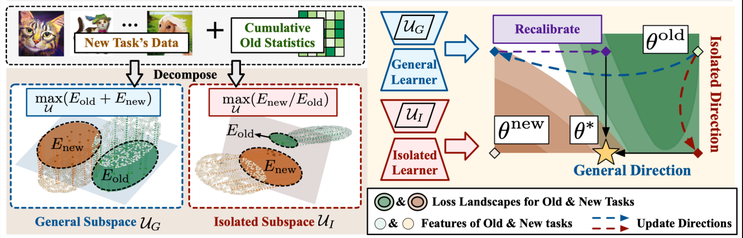

Analysis: **Fixing LoRA down-projection** makes adaptation to new tasks and interference with old tasks controllable:

$$\Delta\mathbf{Y} \triangleq \mathbf{Y}' - \mathbf{Y} = -\eta \left\|\mathbf{A}\mathbf{X}^\top\right\|_2^2 \frac{\partial \mathcal{L}}{\partial \mathbf{Y}},$$

$$\mathcal{L}(\mathbf{Y}') - \mathcal{L}(\mathbf{Y}) = -\eta \left\|\mathbf{A}\mathbf{X}^\top\right\|_2^2 \left\|\frac{\partial \mathcal{L}}{\partial \mathbf{Y}}\right\|_2^2 + o(\|\Delta\mathbf{Y}\|).$$

Discussion: *When fixing LoRA down-projection, the impact of a LoRA update on the loss is governed by **the projection energy** of the task features onto the down-projection's row subspace.*

Solution: This motivates **a task-data-driven decomposition** of the update space into two down-projection subspaces:

(1) **A general subspace** that yields high projection energy across both old and new tasks, capturing transferable directions;

(2) **An isolated subspace** that exhibit largest new-to-old relative energy, identifying truly specific directions for new tasks.

Low-rank Decomposition and Adaptation (LoDA)

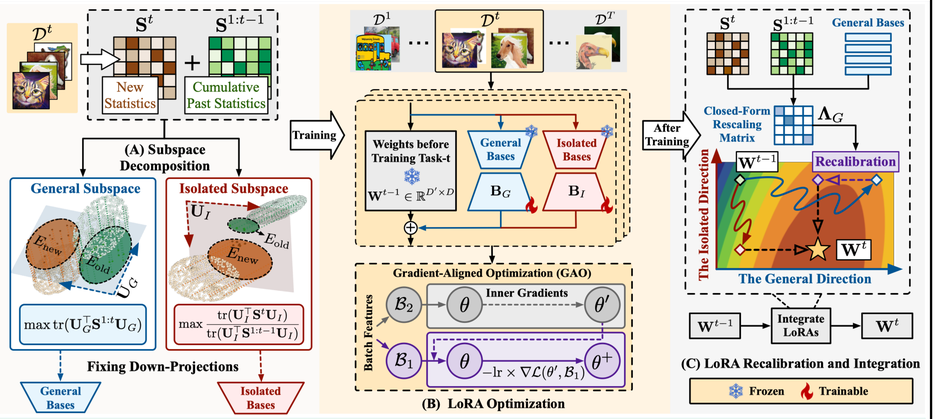

(A) Task-Driven Decomposition

(1) **General subspace**: we seek r orthonormal bases $\mathbf{U}_G$ that achieve a maximal projection energy on both old and new tasks.

$$\mathbf{U}_G = \arg\max_{\mathbf{U}^\top\mathbf{U}=\mathbf{I}_r} \Big(\underbrace{\|\mathbf{X}^t\mathbf{U}\|_F^2}_{E_{\text{new}}} + \underbrace{\textstyle\sum_{i=1}^{t-1} \|\mathbf{X}^i\mathbf{U}\|_F^2}_{E_{\text{old}}} \Big)$$

(2) **Isolated subspace**: we select the r-dimensional isolated directions $\mathbf{U}_I$ by explicitly maximizing the ratio between (i) the projection energy of the new task and (ii) the accumulated energy of all previous tasks.

$$\mathbf{U}_I = \arg\max_{\mathbf{U}\in\mathbb{R}^{D\times r}} \underbrace{\|\mathbf{X}^t\mathbf{U}\|_F^2}_{E_{\text{new}}} \Big/ \underbrace{\Big(\textstyle\sum_{i=1}^{t-1} \|\mathbf{X}^i\mathbf{U}\|_F^2\Big)}_{E_{\text{old}}}$$

(B) Closed-Form Calibration for the General Branch

Directly merge the holistic general update leads to **uncontrollable feature drift**: *How to approximate a feature-level joint optimum along the general direction?*

$$\min_{\mathbf{B}_G^{(j)\star}} \lambda \left\|\mathbf{X}^t(\mathbf{B}_G^{(j)\star}\mathbf{A}_G^{(j)})^\top - \mathbf{X}^t(\mathbf{B}_G^{(j)}\mathbf{A}_G^{(j)})^\top\right\|_F^2 + \sum_{i=1}^{t-1} \left\|\mathbf{X}^i(\mathbf{B}_G^{(j)\star}\mathbf{A}_G^{(j)})^\top\right\|_F^2.$$

Minimizing **joint feature optimization error** of both old and new tasks.

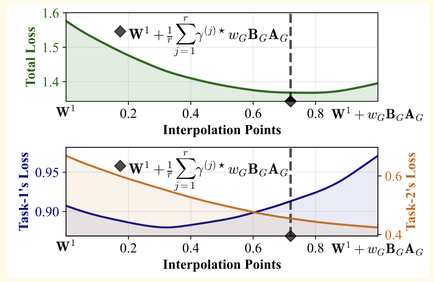

Loss values along the general branch.

EXPERIMENTS

Table 1: Experiment results of LoDA on representative CL benchmarks.

Method	Venue	FR	10S-ImageNetR $\mathcal{A}_{Last}\uparrow$	10S-ImageNetR $\mathcal{A}_{Avg}\uparrow$	10S-ImageNetA $\mathcal{A}_{Last}\uparrow$	10S-ImageNetA $\mathcal{A}_{Avg}\uparrow$	10S-CIFAR100 $\mathcal{A}_{Last}\uparrow$	10S-CIFAR100 $\mathcal{A}_{Avg}\uparrow$	10S-CUB $\mathcal{A}_{Last}\uparrow$	10S-CUB $\mathcal{A}_{Avg}\uparrow$
L2P (Wang et al., 2022b)	CVPR'22	✗	$72.34_{\pm 0.17}$	$77.36_{\pm 0.64}$	$44.04_{\pm 0.93}$	$51.24_{\pm 2.26}$	$84.06_{\pm 0.88}$	$88.26_{\pm 1.34}$	$67.02_{\pm 1.90}$	$79.62_{\pm 1.60}$
DualPrompt (Wang et al., 2022a)	ECCV'22	✗	$69.10_{\pm 0.62}$	$74.28_{\pm 0.66}$	$53.19_{\pm 0.74}$	$64.59_{\pm 0.08}$	$86.93_{\pm 0.24}$	$91.13_{\pm 0.32}$	$68.48_{\pm 0.47}$	$80.59_{\pm 1.50}$
CODAPrompt (Smith et al., 2023)	CVPR'23	✗	$73.31_{\pm 0.50}$	$78.47_{\pm 0.53}$	$52.08_{\pm 0.12}$	$63.92_{\pm 0.12}$	$83.21_{\pm 3.39}$	$87.71_{\pm 3.17}$	$77.23_{\pm 1.12}$	$81.90_{\pm 0.85}$
InfLoRA (Liang & Li, 2024)	CVPR'24	✗	$74.75_{\pm 0.64}$	$80.67_{\pm 0.55}$	$49.20_{\pm 1.12}$	$60.92_{\pm 0.61}$	$86.75_{\pm 0.35}$	$91.72_{\pm 0.15}$	$70.82_{\pm 0.23}$	$81.39_{\pm 0.14}$
SD-LoRA (Wu et al., 2025b)	ICLR'25	✗	$77.34_{\pm 0.35}$	$82.04_{\pm 0.24}$	$55.96_{\pm 0.73}$	$64.95_{\pm 1.63}$	$88.01_{\pm 0.31}$	$92.54_{\pm 0.18}$	$77.48_{\pm 0.20}$	$85.59_{\pm 0.44}$
Bi-LoRA (Zhu et al., 2025)	CVPR'25	✗	$77.95_{\pm 0.14}$	$81.52_{\pm 0.26}$	–	–	$87.46_{\pm 0.76}$	$92.50_{\pm 0.62}$	–	–
PLAN (Wang et al., 2025b)	ICCV'25	✗	$75.25_{\pm 0.42}$	$80.41_{\pm 0.56}$	–	–	$87.54_{\pm 0.31}$	$92.21_{\pm 0.35}$	–	–
LoRA-P&M (Qiu et al., 2025)	NIPS'25	✗	$79.95_{\pm 0.18}$	$85.29_{\pm 0.93}$	$56.57_{\pm 0.78}$	$65.35_{\pm 1.81}$	$88.45_{\pm 0.35}$	$92.89_{\pm 1.13}$	$78.29_{\pm 0.50}$	$83.39_{\pm 0.61}$
CoSO (Cheng et al., 2025)	NIPS'25	✗	$81.10_{\pm 0.39}$	$85.56_{\pm 0.13}$	–	–	$88.77_{\pm 0.16}$	$92.99_{\pm 0.23}$	–	–
LoDA (Ours)	–	✗	$\mathbf{81.93}_{\pm 0.20}$	$\mathbf{86.90}_{\pm 0.40}$	$\mathbf{62.59}_{\pm 0.64}$	$\mathbf{70.87}_{\pm 1.61}$	$\mathbf{90.47}_{\pm 0.06}$	$\mathbf{93.46}_{\pm 1.42}$	$\mathbf{81.74}_{\pm 0.78}$	$\mathbf{89.35}_{\pm 0.98}$
SLCA (Zhang et al., 2023)	ICCV'23	✓	$79.35_{\pm 0.28}$	$83.29_{\pm 0.46}$	$61.05_{\pm 0.63}$	$68.88_{\pm 2.31}$	$91.26_{\pm 0.37}$	$94.29_{\pm 0.92}$	$84.68_{\pm 0.09}$	$90.77_{\pm 0.79}$
SSIAT (Tan et al., 2024)	CVPR'24	✓	$79.38_{\pm 0.59}$	$83.63_{\pm 0.43}$	$62.43_{\pm 1.63}$	$70.83_{\pm 1.63}$	$91.35_{\pm 0.26}$	$94.35_{\pm 0.60}$	$88.75_{\pm 0.38}$	$93.00_{\pm 0.90}$
VQ-Prompt (Jiao et al., 2024)	NIPS'24	✓	$75.68_{\pm 0.23}$	$80.02_{\pm 0.18}$	–	–	$90.27_{\pm 0.06}$	$93.10_{\pm 0.84}$	$86.47_{\pm 0.40}$	$91.37_{\pm 0.54}$
DIA (Li et al., 2025a)	CVPR'25	✓	79.03	85.61	61.69	71.58	90.80	94.29	86.73	93.21
MACIL (Wu et al., 2025a)	ICML'25	✓	$81.88_{\pm 0.07}$	$85.95_{\pm 0.27}$	$64.14_{\pm 0.58}$	$71.45_{\pm 1.35}$	$91.94_{\pm 0.17}$	$94.43_{\pm 0.79}$	$90.52_{\pm 0.13}$	$93.93_{\pm 0.47}$
LoDA (Ours) + CA	–	✓	$\mathbf{82.55}_{\pm 0.55}$	$\mathbf{87.18}_{\pm 0.42}$	$\mathbf{66.71}_{\pm 0.75}$	$\mathbf{73.89}_{\pm 1.22}$	$\mathbf{92.15}_{\pm 0.21}$	$\mathbf{94.70}_{\pm 1.16}$	$\mathbf{90.67}_{\pm 0.17}$	$\mathbf{93.97}_{\pm 0.56}$

Table 2: Comparison with different **task isolation methods** on two benchmarks.

Dataset	Method	$\mathcal{A}_{Last}\uparrow$	$\mathcal{A}_{Avg}\uparrow$
10S-ImageNetR	Random Orthogonal Bases	$68.23_{\pm 0.18}$	$79.05_{\pm 0.62}$
	Adam-NSCL (Wang et al., 2021)	$74.50_{\pm 0.77}$	$82.29_{\pm 1.12}$
	InfLoRA (Liang & Li, 2024)	$75.15_{\pm 0.37}$	$82.57_{\pm 0.84}$
	Relative Energy Maximization (Ours)	$\mathbf{79.22}_{\pm 0.50}$	$\mathbf{85.22}_{\pm 0.73}$
10S-ImageNetA	Random Orthogonal Bases	$53.48_{\pm 1.47}$	$64.34_{\pm 1.86}$
	Adam-NSCL (Wang et al., 2021)	$55.95_{\pm 1.84}$	$66.94_{\pm 2.03}$
	InfLoRA (Liang & Li, 2024)	$57.10_{\pm 0.96}$	$67.55_{\pm 1.94}$
	Relative Energy Maximization (Ours)	$\mathbf{59.89}_{\pm 0.68}$	$\mathbf{68.97}_{\pm 2.03}$

Figure 1: Projection magnitude and relative projection energy values across ViT layers.

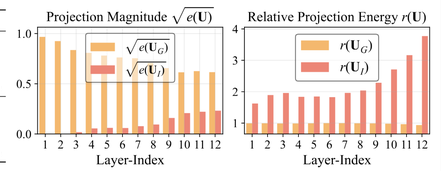

Analysis: *Why our **relative energy maximation objective** for building isolated subspace perform better than existing null-space-based methods?*

Task distributions are correlated, **the estimated old null space can be nearly inactivate on new tasks**.

$$r^t(\mathbf{U}) \triangleq \frac{\|\mathbf{X}^t\mathbf{U}\|_F^2/\|\mathbf{X}^t\|_F^2}{\sum_{i=1}^{t-1}\|\mathbf{X}^i\mathbf{U}\|_F^2/(\sum_{i=1}^{t-1}\|\mathbf{X}^i\|_F^2)},$$

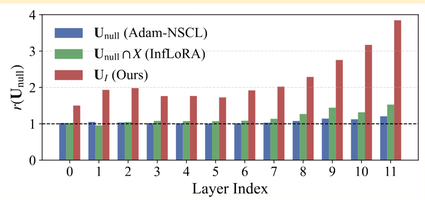

We observe $r^t(\mathbf{U}_{\text{null}}) \approx 1$ of null space $\mathbf{U}_{\text{null}}$, supporting our analysis.

CONTACT INFORMATION

If you are **interested in my work or would like to collaborate**, feel free to add me on WeChat or contact me at lingfenghe077@gmail.com.

WeChat | Personal Website | Github Page | Google Scholar